Structural Analysis of Historic Construction – D'Ayala & Fodde (eds)
© 2008 Taylor & Francis Group, London, ISBN 978-0-415-46872-5

The great hall of the Trajan Markets throughout the centuries

L. Ungaro & M. Vitti
Office for Trajan's Markets Museum and Imperial Forum, Rome, Italy

E. Speranza
Architect, Rome, Italy

ABSTRACT: The paper illustrates ongoing research on the great hall of the Trajan Markets in Rome, led by the Office of the Trajan Markets Museum. The research has been conducted during the restoration and seismic upgrading of the monuments.

The first part of the work is devoted to a description of structural layout and archaeological evidences, allowing some reconstructive hypothesis in different periods of the life of the monument. Among these, the roman configuration is examined under the point of view of its mechanical behaviour, using the method of funicular polygons. The analysis is carried out in static conditions and simulating the historical earthquakes which the monument (in its original configuration) undergone.

The paper discusses the structural safety margin of the Roman vault in relation to the mechanical effectiveness of different structural elements, and finally some conclusions are drawn on the present state of the Vault.

1 THE GREAT HALL OF TRAJAN'S MARKETS

1.1 *Introduction to the Monument*

The Great Hall of the Trajan's Markets is one of the most impressive monuments of the Imperial Period still standing in the very heart of Rome.

Its architectural and structural layout, likewise the one of the whole Complex of the Markets, is attributed to Apollodoro from Damascus, architect directly charged by Trajan Emperor to carry out the ambitious and monumental project of Trajan Forum.

The architectonic and structural layout of the Hall is innovative for the construction technique of the period. Previous researches on similar typological schemes in the roman architecture carried out by several authors (Giovannoni 1913, Bianchini 1991, Lancaster 2000, Vitti 2007) have stressed the presence of significant innovations compared to other monuments of the period.

1.2 *The Great Hall today: architectonic and structural layout*

The Great Hall is featured by a planimetric rectangular shape. A monumental concrete vault, spatially articulated through six consecutive cross vaults, covers a double-height space; the space between the pillars is covered by barrel volts. Along both sides of the Hall is a system of "*tabernae*" placed on two storeys, structurally shared by thick concrete walls.

The Vault is supported, at the second storey, by isolated pillars, and connected to the rest of the structure by slender arches (Figure 1, left).

The choice of materials used in the construction process was made on the basis of the structural function of each element as well as of the relative strength required for each of them.

The seven pillars on both side of the hall are built up using two different techniques: the lower part is realised by two travertine ashlars blocks measuring $75 \times 90 \times 150$ cm ($2{,}5 \times 3 \times 5$ roman feet).

The superior block was originally shaped as a corbel outstanding inward the vault. At present only one corbel is left of the original system, and this is placed on the south facade wall (Figure 1, right).

The masonry portion over the travertine blocks is made up of roman concrete, with external red brickwork leaf, starting from a horizontal layer of *bipedales* elements (59 cm, two roman feet).

The barrel vaults between pillar and pillar are realised in concrete with different assortment from springing to the keystone: haunches are mainly made up of brick fragments, while at the crown they are replaced by lighter tuff fragments. The concrete of the central part of the vault is made of grey mortar with black aggregates and yellow tuff, used as *coementa*.

Figure 1. Left: view of the vault of the Great Hall. Right: south-west pillar with travertine corbel.

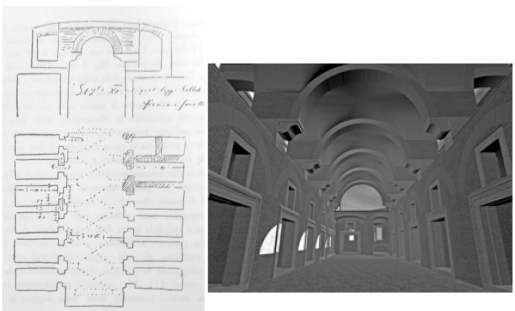

Figure 2. Left: sketch by Marciana Library. Right: 3d reconstruction by M. Bianchini (2003).

The original thickness of the vault to the keystone was of 30 cm and the flat extrados was used as terrace with an articulated waterproofing system (Ungaro-Vitti 2001).

1.3 *The Great Hall through the centuries*

The original layout of the Roman vault can be reconstructed through archaeological data and, most of all, through old paintings and sketches as those by Giulio Romano (*Lapidazione di S. Stefano* 1520–1546), Sallustio Peruzzi (Florence, Uffizi Museum XVIth century), and one more preserved in the Marciana Library (XVIth) (Figure 2, left).

Indications and evidences provided by this research type, critically analysed and put side by side, enable to formulate the hypothesis according to which the six cross vaults into which the main vault is shared, were originally divided by transversal ribs made of *sesquipedales* (45 cm), shaped as round arches and springing by the travertine corbels (Bianchini-Vitti 2003) (Figure 2, right). Apart from these, the other elements of the vault, existing in the roman period, are still preserved.

The Medieval period is little documented under an archaeological point of view. It is reasonable to suppose that the Great Hall did not undergo any significant work until the Renaissance; since the space was continuously used.

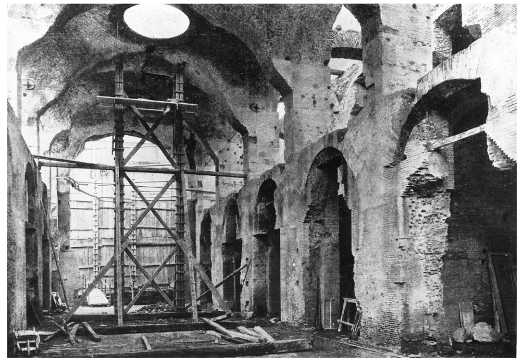

Figure 3. The Great Hall in 1929 during restoration works.

At the end of the XVIth century, the Complex was turned into a Convent (Santa Caterina from Siena) and heavy alterations to the structure were carried out by the Santa Caterina's nuns, in order to adapt the space to their needs. The space of the Great Hall was divided in two storeys by a horizontal structure at the level of lateral corridor.

Moreover in order to use the above space, the travertine corbels were all cut off, except from those included in the south facade.

Heavy removals of material were made in proximity of pillars (up to a height of 1, 50 m from pillar basis), so as to reshape the vault intrados.

Transversal arch-ribs were also removed. In order to obtain a covered space, the lateral corridors were sheltered by thin cross vaults between the contrast arches.

In this period, a rough round opening (more likely opened in a previous phase), was reshaped with a regular circular array of bricks.

In 1926 the Great Hall underwent new important works. Under the scientific direction of Corrado Ricci, the second floor and the lateral cross vaults in the side corridors were demolished and the circular opening walled up (Ricci 1929). Further strengthening works, regrettably little documented, were also carried out to bring back the structure to its "supposed" Roman configuration (Figure 3).

Longitudinal (north-south) metallic ties were placed at vault springing, anchoring the edge barrel vaults to the structures behind. Similarly, another couple of ties were inserted in a new thick concrete layer above the roman pavement, in order to anchor the north façade to the rest of the monument.

In addition to this the pillars were also tied through metallic rings, so as to contain the worsening of a crack pattern, even visible from pictures of the period.

Massive repairs, even with bricks or rough material, were carried out on cracks at intrados of the vault, particularly to the longitudinal one, interesting the entire length of the hall.

In 2000 the cracked pillars were strengthened, once having removed the metallic rings. The works provided the insertion of a consistent number of stainless bars, inclined through the pillar width.

The restoration started in 2004 and recently concluded, was carried out to improve the seismic performance of the monument, following the classification of Rome as seismic prone area in 2003.

Metallic ties were placed at all levels of the lateral *tabernae*, and the vault was tied by a system of horizontal bars, inserted in the vault thickness just over the crown level, with extremities anchored to the contrast arches. The longitudinal stiffness of the vault was also increased by a couple of crossed iron bars, in the spaces between contrast arches.

A more accurate description of these works is provided in a parallel work by Croci et al., in the Proceedings of this same Congress.

1.4 *Archaeological evidences of structural performance*

To sum up the structural elements characterising the roman configuration, can be listed ad follows:

- Ashlars blocks at pillar basis with corbels inward-outstanding the vault;
- Transversal arch ribs, at vault intrados aligned with lateral pillars (at present lost);
- Contrast side arches connecting the vault to the lateral structures (*tabernae*).

Beyond these, some more aspects concerning the support structures require to be introduced in order to have a clearer view of the structural layout.

In particular it deserves to be mentioned the presence of clamp marks, systematically placed on three sides of each pillar (two on each lateral side, one on the external face), through travertine blocks joints.

The clamps measures, (reconstructed by the visible marks) were 28–33 cm high and 13 cm width.

Figure 7, right, shows the picture of a pillar with the drawings of its three elevations. The clamps signs are clearly visible.

So far we do not know the material by which clamps were made, if iron or wood. It can also be supposed the presence of a metallic ring tie, keeping together the clamps on each pillar.

However it can be made the hypothesis according to which clamps would have been placed following the pillar construction. If different, they would have been inserted in the inner core of travertine blocks, rather than on their external faces. The clamps were reasonably placed with a structural (static or seismic) purpose, and their feasible function is examined and discussed in the following paragraphs dedicated to the mechanical performance of the vault.

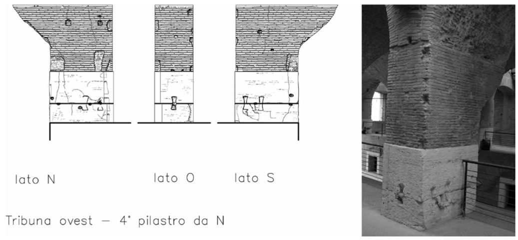

Figure 4. Left: Elevation of three sides of a pillar, with visible clamps and damage pattern. Right: View of the same pillar.

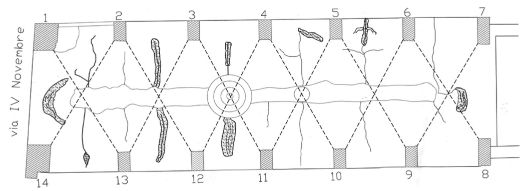

Figure 5. Survey of crack pattern observed at vault intrados.

1.5 *Damage and crack pattern observed*

The structural damage involving the vault is certainly rather old, as it was documented since 1930 works, and this was the cause of specific strengthens then implemented.

During recent restoration works (2004), the vault structure was analysed in detail and the crack pattern observed, once removed a thick plaster of 1930, carefully documented by photographs and surveys.

Extensive damage was documented on the vault intrados (Figure 5). The most important crack, filled up during 1929–1930 works, is longitudinal (North-South) at crown, involving the whole length of the vault.

Similar cracks were also present at the intrados crown of lateral barrel vaults, with damage intensification on those towards the north façade. The crack pattern involves also pillars, both on travertine blocks and on superior concrete portion. The cracks are vertical, and placed on the longer sides of the pillars and particularly on the internal edge. Diffused cracks are also present in the upper zone where the original vault shape was cut off (Figure 4, left).

2 THE MECHANICAL BEHAVIOUR

2.1 *Method of analysis*

Parallel research work similarly aimed, included in the proceedings of this same Conference, analyse the vault

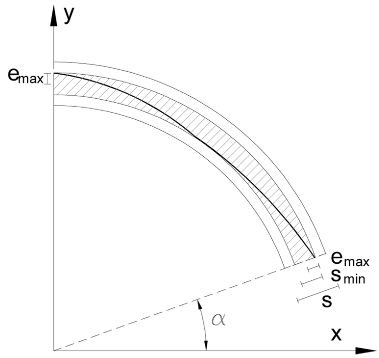

Figure 6. Minimum thickness arch and funicular polygon closest to the axis line.

of the Great Hall using Finite Elements, conceptually based on the elastic theory of materials (Croci et al., 2008). An alternative criterion, pursued in this paper, is the analysis through the static theory applied to masonry arches.

The arch mechanical safety is defined, according to a geometrical approach, through the funicular polygon whose construction was early developed by A. Mery (1840). A three pin arch is the static determinate scheme for drawing the thrust line, as well as writing equilibrium equations. The arch stability is guaranteed only when the thrust line is always contained within the arch thickness.

In addition to this, among the possible infinite polygons which can be found out along the arch ring, it is possible to identify the *real* one assumed by the arch, as formulated by J. Heyman 1982 (Heyman 1982).

This is identified as the one closest to the axis line of the arch. The ideal arch with intrados and extrados both tangent to this polygon, is defined as *minimum thickness* arch (Figure 6).

In order to maintain all joints of the arch always in compression, Heyman's *middle third rule*, requires for the arch equilibrium that the line of pressure, or thrust line, is always internal to the third middle of each joint width.

Beyond this, two more thrust lines can be defined, which represent the two extreme configurations of the funicular polygon. The *minimum thrust line* is associated with a polygon passing at extrados at the crown and at the intrados, at haunches. When the pillars are not strong enough for containing the thrust, the whole structure onsets on to a failure mechanism of rigid bodies (Figure 7, a). This limit configuration of the polygon is typically the one assumed in presence of slender pillars. Conversely the *maximum thrust line* is associated with a polygon passing at intrados at crown, and at abutments at extrados (Figure 7, b). This polygon is more often the one assumed in presence of high

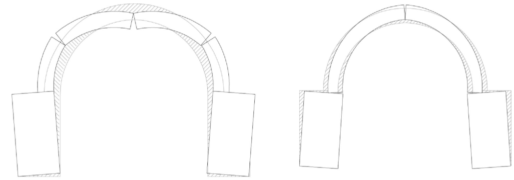

(a) (b)

Figure 7. Failure mechanisms associated with minimum (a) and maximum (b) thrusts. The hinges position depends on geometric characteristics and on load applied to the arch.

lateral thrusts, or even in presence of a metallic ties placed at abutments.

The calculation of the funicular polygon according to the above approach was translated into a computer program in 1997 by one of the authors (Ceradini, Sguerri, Speranza 1997) and then applied to the ashlars vaults of the historic Sassi of Matera, within a research work for the Code of Practice of the same town, leaded by A.Giuffrè (1997).

The capability of the program is that it can calculate (even in presence of a seismic action) any type of arch, of any geometry, which can be shared in a real (or ideal) number of n elements (and $n+1$ joints).

Once the weights and acting loads have been calculated, the program computes the Resultants ($Rx_{1,3}$ and $Ry_{1,3}$) at abutments, through equilibrium equations of a three pin arch. The position of the three pins (m_1,m_2,m_3) among the $n+1$ joints is arbitrary, and is governed by a specific coefficient ξ, for each of the three hinges.

Finally, further segments of the polygon, starting from the left side hinge, are calculated as far as the last joint of the arch.

The safety factor of the arch is defined as:

$$\eta = \frac{s}{s_{\min}} \tag{1}$$

Where s_{min} is given by:

$$s_{\min} = e_{\max} - e_{\min} \tag{2}$$

and e_{max} and e_{min} are the maximum and minim eccentricities of the thrust line under calculation (Figure 6).

The program is interactive with the user, so that he can decide the joints where to locate the three hinges, and their position along each joint.

Once optimized the safety factor, through an iterative process the of the arch, and hence univocally identified the funicular polygon, the program provides the calculation of stresses along the joints and checks that the ratio between lateral (T_i) and normal (N_i)

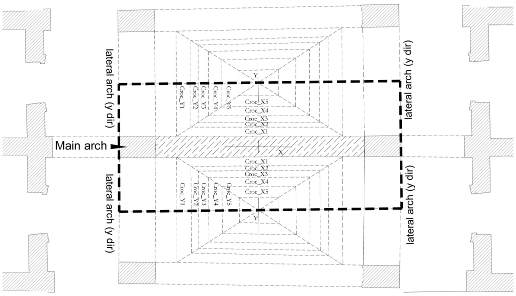

Figure 8. Vault span taken in exam in the model.

forces acting on each joint, does not overcome the friction coefficient f:

$$\frac{T_i}{N_i} \leq f \qquad (3)$$

Stresses on each joint are finally calculated assuming a material with no tensile strength.

2.2 *The model of the Great Hall*

Following a similar approach pursued for analysing the Basilica of Maxentius, leaded by Giavarini et al. (2005) the static of the cross vault of the Trajan Markets has been analysed using the method above introduced, having preliminarily defined the geometric and static model.

A central span of the vault has been taken in exam, realized by a central arch ring with side pillars, (90 cm width), four orthogonal mid-barrel vaults and two lateral mid cross-vaults (Figure 8).

The central arch aligned with side pillars has been assumed as the main structural system conveying the vertical loads and thrusts of the adjacent vault portions to the ground.

The main arch has been modelled by virtual joints, while those really existing at pillars have been modelled by reproducing their exact position: at partition between concrete and travertine blocks, and between the two travertine blocks (Figure 9).

Two geometric configurations at extrados have been assumed in the analysis for the main arch, so as to take in exam the presence and the absence of the transversal rib documented in the roman configuration, introduced in §1.3. Figure 9 shows the model relative to the roman layout, without transversal rib.

Moreover, travertine corbels are present at arch springing and these are joined with the travertine ashlars block of the pillars.

The difference of material between supports (travertine) and vault (concrete) has been modelled in the analysis by associating different specific weights (24 KN/mc and 15 KN/mc respectively).

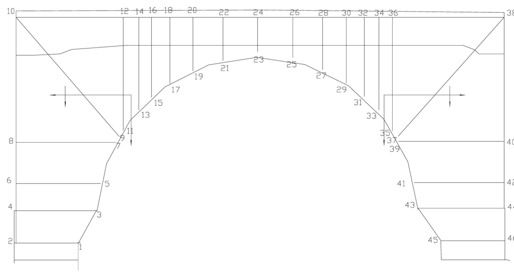

Figure 9. Geometric model of the main arch relative to the roman configuration, without transversal rib.

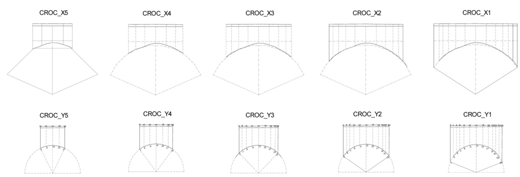

Figure 10. Virtual arches forming the lateral cross vaults.

A distributed load has been applied to the extrados of the vault (6 KN/mq) so as to take in consideration the presence of the waterproofing layer (§1.2), brickwork pavement and an additional overload.

Similarly to the above approach, a geometric model has been developed for the orthogonal barrel vault, divided by 13 virtual joints, with same distributed load assumed for the main arch. The assumed thickness at keystone (smaller than in the present situation) for the roman configuration is 0.83 m.

According to the same criterion, the cross vault has been divided into virtual arches in both directions x, y, geometrically defined by progressively lower spans of the main and lateral barrel vaults (Figure 10).

In a first step of the analysis, these structural elements have been analysed independently from each other, so as to obtain the vertical resultant R_{y1} and R_{y3} at springing, and the horizontal thrusts (R_{x1} and R_{x3}).

The funicular polygons found out for the orthogonal barrel vault (y dir) is sketched in Figure 11, left.

For the cross vault, independent polygons have been calculated for each of the ideal arches illustrated in Figure 10.

The resultants obtained for each of them have been applied to the diagonal arch of the same vault. Figure 11, right, highlights the funicular polygons of the diagonal arch, relative to minimum arch width and minimum thickness conditions.

When analysing the stability of each of the above elements independently from each other (barrel vaults and cross vault) and from supports conditions, the safety coefficient (associated with minimum thickness polygons), are considerably high: greater than 10 for

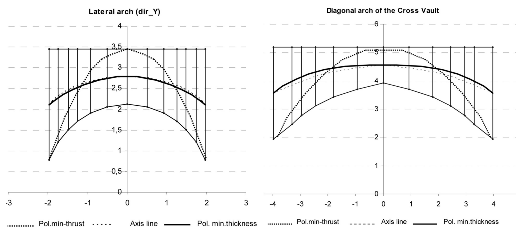

Figure 11. Funicular polygons of orthogonal barrel vault (left) and diagonal arch of the cross vault (right) relative to the present configuration.

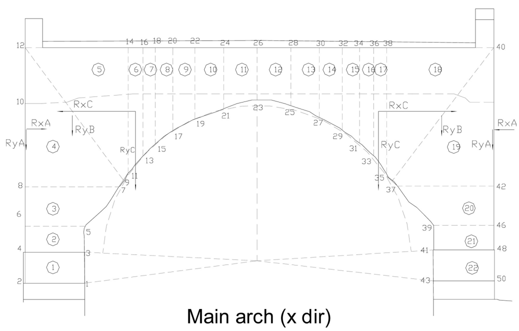

Figure 12. Final model of main arch with applied loads relative to orthogonal barrel vaults, cross vaults and contrast arches.

the barrel vault and greater than 5 for the diagonal arch, with joints in both cases always in compression.

In addition to the above, a third sub-system has been introduced, consisting in contrast arches lateral to the pillars, as described in §1.2.

The resulting model of the vault combines, in the main arch, the action produced by each individual sub-system.

One assumption is that, for the overall equilibrium of the structure, the single elements (orthogonal vaults and cross vault) behave minimizing the thrusts, while the contrast arches maximizing the horizontal action.

The final model of the vault is determined by applying the resultants of sub-systems (R_{yB};R_{xC};R_{yC} R_{xA};R_{yA}) to the main transversal arch, as shown in Figure 12.

2.3 *The mechanical behaviour of the Vault in the Roman period under static loads*

The configurations analysed in the present work, are the following:

R1 Vault *without* transversal arch and lateral arches;
R2 Vault *without* transversal arch *with* contrast arches;
R3 Vault *with* transversal arch, *without* contrast arches;
R4 Vault *with* transversal arch and contrast arches.

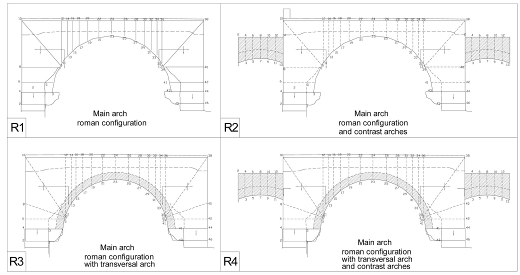

Figure 13. Four configurations assumed for the Roman period.

Each of the above configurations, corresponding to specific load conditions and geometric layouts, are sketched and labelled in Figure 13.

It is worth noticing that all the configurations show a regular arch ring, without removals occurred in the 16th–17th century.

The four configurations are all examined so as to assess the role exerted by two constructive elements like contrast arches and transversal (hypothetical) rib.

In determining the mechanical behaviour of the vault, the first step was to find out which polygon, among the infinite possible congruent with load and geometric conditions, was to be assumed.

Figure 14 shows two different polygons processed for the main arch in absence of contrast arches and rib. The minimum thrust polygon corresponds to e limit equilibrium ($\eta = 1$), showing very high compressive values at crown (more than 10 KN/cmq) and at haunches. Similar configurations of the thrust line (minimum thrust) have been found out for the other roman layout of Figure 13: the overall equilibrium is assured, though joint sections (at crown and haunches) result only partially working. These clearly correspond to limit equilibrium states.

Consequently, different equilibrium layouts have been looked for, so as to find out feasible configurations associated with higher safety coefficients, as well as stresses compatible with material strength: the minimum-thickness polygon has been reasonably assumed as the one adopted from the structure to convey the loads to the ground.

The second polygon shown in Figure 14 (minimum thrust, associated with R1 layout), shows rather high compressive stress at crown (0.17 KN/cmq), with a notable sliding coefficient between the two travertine blocks (joints 2 and 24): 0.46. Moreover high compression is present at keystone extrados, while intrados is not working and this is compatible with the onset of a crack. This yield to conclude that the equilibrium of this configuration, without any structural device system, show very poor equilibrium conditions and hence can be considered very unlikely.

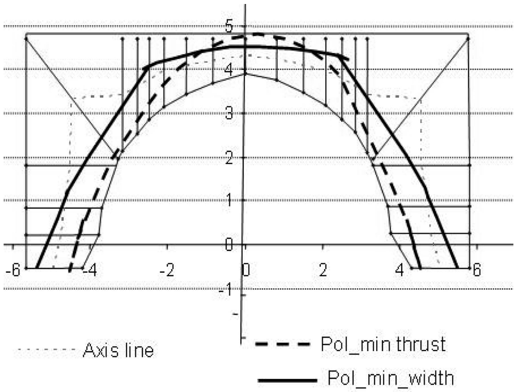

Figure 14. Polygons calculated for the main arch (layout R1) without transversal rib and contrast arches (worst situation).

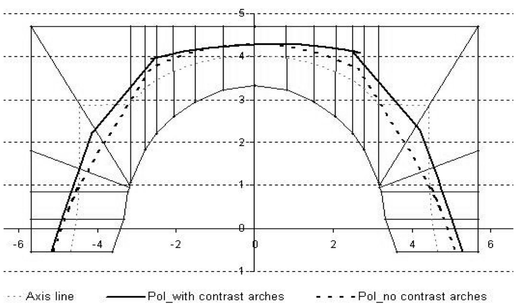

Figure 15. Polygons obtained for the main arch in presence of transversal arch, without and with contrast arches (layout R3, R4).

Similarly, minimum thickness thrusts (relative to the layouts R2, R3, R4) have been processed.

Figure 15 shows the polygons obtained in presence of the transversal rib without and with contrast arch (layouts R3, R4).

One can note that the line of pressure associated with the second condition (R4) is closer to the axis line and less inclined at pillar springing. In this case lower sliding coefficients between the two travertine blocks are obtained.

The results obtained for the 4 configurations of Figure 13, are summarised in Table 1. The same values are plotted in the histogram of Figure 16, left.

The results achieved for the roman configuration yield to conclude that:

- The presence of contrast arches, slightly improve the mechanical performance of the vault, mitigating the risk of sliding between the two travertine blocks. However, in absence of transversal rib, high compressive values are present at pillars basis, at extrados, while internal face is not working;
- The presence of the transversal arch improves the static performance of the vault the keystone at intrados still is not working.
- The presence of both transversal rib and contrast arches represents the best configuration, under a mechanical point of view. The sliding coefficient is acceptable (lower than 0.3), while the section at keystone is partially reacting, and this is still compatible with the onset of a longitudinal crack.

One hypothesis which can be formulated, is that following the construction of the vault (at the same time of lateral arches), and the following onset of a longitudinal crack at crown, special devices would have been on purpose placed at pillars bases (between travertine blocks) in order to prevent their mutual sliding. This is confirmed both in absence and presence of the transversal arch; although in this second case the risk of sliding would have been more inhibited.

2.4 *Strongest historic earthquakes experimented by the Vault*

Produce Among the strongest historic earthquakes which hit Rome in the Imperial period, it deserves to be mentioned the one of 113 a.C. which produced serious cracks to the Trajan Column on the north side of the Forum. Two hundred and half years later, in 443 a.C., one stronger event hit the town, generating several damage on many monuments (probably in a state of decay following the Goth's invasion). Among the damaged buildings, it can be mentioned the Colosseum which was repaired and its works reminded on the external wall (Lanciani 1917, Galli 1906). Further seismic events occurred in 448 a.C. and 508 a.C, the latter with cracks on Coliseum. We have no direct information on damage to Trajan's Markets, though it is very plausible that these structures were injured in a similar way to other contemporary monuments of the period.

Among these, the strongest documented earthquake is the one of 443, with local associated MCS intensity VIII.

This earthquake was then assumed to simulate the structural behaviour of the vault of the Great Hall. The MCS intensity has been turned into PGA using traditional conversion methods (Margottini, 1993).

The polygons obtained with the effect of the seismic action ($a/g = 0.2$, acting in the $-x$ direction), are plotted in Figure 17. The structural configuration is the one with transversal rib, with and without contrast arches.

One can note that in presence of the earthquake, the polygon bends in the direction opposite to the one of the earthquake, with a consequent more inclined resultant on the external pillar (in this specific case left pillar). A consequence of this is that higher sliding coefficients will be expected, and this in turn

Table 1. Results obtained for the 4 Roman configurations.

		Roman arch				
		Hinges position (ξ)	η	Sliding coefficient	Max compression (KN/cmq)	Parzialized joints
R1	without transversal arch; without lateral arches	0,8;0.8;0.8	1,62	0,45	0,17	all upper part
R2	without transversal arch; with **lateral arches**	0.65; 0.55; 0.65	1,88	0,35	0,10	several joints
R3	**with transversal arch**; without lateral arches	0,73;0.7;0.73	2,16	0,40	0,09	crown
R4	**with transversal arch**; without lateral arches	0,6;0.67;06	2,72	0,29	0,06	crown

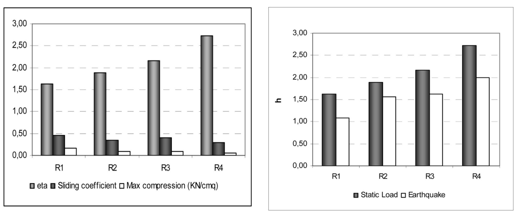

Figure 16. Left: histogram of h, sliding coefficient and compressive stresses obtained for the 4 different configurations of the roman vault. Right: Histogram comparing the safety coefficients obtained for the 4 configuration of the vault, under static and seismic loads.

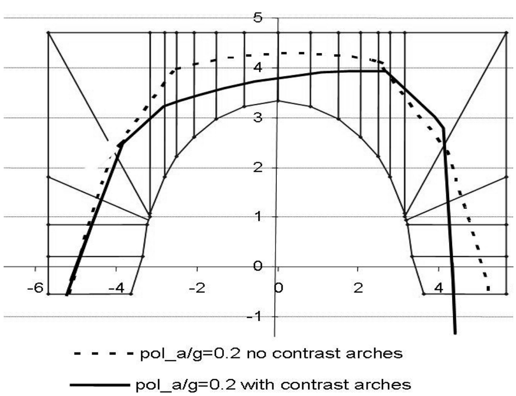

Figure 17. Polygons obtained in presence of transversal rib, without and with contrast arches, with seismic action $a/g = -0.2$.

determines higher risk of sliding between travertine blocks.

The results obtained in presence of earthquake, for the 4 different configurations examined under static loads, are shown in Table 2. Figure 16 (right) compares the safety coefficients obtained for the 4 layouts of the vault under static and seismic loads.

Similarly to the static case, one can note that passing from the former to the latter configuration, the safety coefficients (η) of the vault tends to increase. However the first configuration is very close to a limit equilibrium ($\eta = 1.09$). Conversely, when the two structural elements are both present, the safety coefficient becomes equal to 2.

The sliding coefficients show in all cases values considerably high, particularly in layouts 1 and 3 (0.59 and 0.52 respectively). This yields to conclude that the earthquake severity experimented in 443 a.C., might have onset an initial sliding mechanism between travertine blocks. In addition to this the joints between these blocks are only partially working in compression. The eccentricities varies from (0.58 m of the first case to 0.51 m of the last), so that a pillar portion, facing the internal side of the vault, is not working. This might have produced the vertical cracks cutting the blocks (which can be observed still now) and the consequent collapse of the travertine corbels.

3 CONCLUSIONS

The results achieved help to focus some crucial point of the vault in its original configuration, as well as to formulate some hypothesis.

- The presence of contrast arches improves the behaviour of the vault both under static and seismic loads. However their contribution in this case is more relevant.
- Similarly, the transversal arch, if really conceived in the original layout of the vault, helps the mechanical performance of the structure.
- The presence of anti-sliding devices on purpose placed between the travertine blocks might have two

Table 2. Results obtained for the 4 Roman configurations under the effect of a seismic action.

		Hinges position (ξ)	η	Sliding coefficient	Max compression (KN/cmq)	Parzialized joints
Rs1	without transversal arch; without lateral arches	0,9;0,4;0,4	1,09	0,59	0,36	haunches and pillar bases
Rs2	without transversal arch; with **lateral arches**	0,8;0,27;0,4	1,56	0,47	0,19	haunches and pillar bases
Rs3	**with transversal arch**; without lateral arches	0,79;0,5;0,32	1,63	0,52	0,12	haunches and pillar bases
Rs4	**with transversal arch**; **without lateral arches**	0,75;0,36;0,4	2,00	0,44	0,11	haunches and pillar bases

order of purposes: they might have been placed following the construction, once the longitudinal crack at crown became visible, in order to prevent the sliding mechanism. Conversely, following a seismic event (more likely the one of 443 a.C.) once some very small displacement between travertine blocks came to the light.

- The action of the earthquake was the possible cause producing the (still visible) vertical cracks, cutting the travertine corbels.

The works realised in the structures in the last 20 years, particularly those of 1996, have completely changed the mechanical behaviour of the structure. In particular, the insertion of metallic bars, within the concrete core of pillars as well as between travertine blocks, has definitively impeded any sliding likelihood, with the drawback of having locally modified the masonry stiffness, and its possibility of adjustment to external solicitations.

Further analysis of the vault taking in exam the alterations to the structure following the roman period are at present in progress, in order to compare the different safety margins from its construction until today.

REFERENCES

Boschi E., Guidoboni E., Ferrari G., Valensise G., Gasperini P. 1997. Catalogo dei forti terremoti storici in Italia dal 461a.C al 1990. vol.2. (ING-SGA). Bologna, Italy. p.644.

Bianchini M. 1991. I Mercati di Traiano. In *Bollettino di Archeologia del Ministero dei Beni Culturali e Ambientali* (8) Marzo-Aprile 1991:102–121.

Bianchini M., Vitti M. 2003. Il Complesso dei Mercati di Traiano alla luce dei recenti restauri e delle indagini archeologiche. La fronte della Grande Aula e il suo sistema scalare. In *Bullettino della Commissione Archeologica Comunale di Roma* (CIV), 2003: 285–306.

Ceradini V., Speranza E., Sgherri L., La Statica delle Volte, 1997. In: *Codice di Pratica per la conservazione dei sassi di Matera*, edited by A.Giuffrè, C.Carocci, La Bautta Editions, Bari.

Croci G., Viskovic A., Bozzetti A., Ungaro L., Vitti M. 2008. The Trajan Markets and their Great Hall – The Conservation Problems and the Structural Intervention for the Improvement of the Seismic Safety. In SAHC .

Galli I. 1906. I Terremoti nel Lazio. In: Stab. Tip. "Pio Stracca" (eds), Velletri.

Giavarini et. Al. 2005. *La Basilica di Massenzio. Il monumento, i materiali, la stabilità,* C. Giavarini (ed.), Roma.

Giovannoni G. 1913. Prototipi di archi rampanti in costruzioni romane. In *Annali della Soc.Ingegneria ed Architettura italiana*. N.10.

Heyman J. 1982. The masonry arch., Ellis Horwood, Chirchester.

Lancaster L. 2000. Building Trajan's Markets 2: the Costruction Process. In *American Journal of Archaeology* (104,4) 2000: 755–785.

Lanciani R. 1917. Segni dei Terremoti negli edifizi di Roma antica. In *Bullettino della Commissione Archeologica Comunale*, Rome.

Margottini C., Molin D., Serva L. 1993. Earthquake intensity vs peak ground acceleration in Italy (unpublished ms).

Mery E. Sur l'equilibre des voutes en berceau. In *Annales des Pontes et Chausses*, 1840.

Ricci C. 1929. *Il Mercato di Traiano*. Roma

Ungaro L., Vitti M. 2001. Sulle pavimentazioni dei Mercati di Traiano. In *Atti del'VIII Colloquio dell'Associazione Italiana per lo Studio e la Conservazione del Mosaico* (21–23 febbraio 2001) F. Guidobaldi & A. Paribeni (eds), Ravenna: 393–414.

Ungaro L, Vitti M. 2007. I Mercati di Traiano affrontano il nuovo millennio. *Forma Urbis* (XII, n. 2) febbraio 2007: 4–15.

Vitti M. 2007. The Sequence of Buildings. In L. Ungaro (ed), *The Museum of the Imperial Forums in Trajan's Market*, Milan: 53–59.